

Contribution to the
XVth International Conference
on High-Energy Physics, Kiev,
U. S. S. R. , August 26-
September 4, 1970

UCRL-20076
Preprint

CONF-700806--46

MASTER

K^{*0} PRODUCTION IN
 K^+d INTERACTIONS AT 12 GeV/c

A. Firestone, G. Goldhaber, and D. Lissauer

August 1970

AEC Contract No. W-7405-eng-48

UCRL-20076

DISTRIBUTION OF THIS DOCUMENT IS UNLIMITED

LAWRENCE RADIATION LABORATORY
UNIVERSITY of CALIFORNIA BERKELEY

DISCLAIMER

This report was prepared as an account of work sponsored by an agency of the United States Government. Neither the United States Government nor any agency Thereof, nor any of their employees, makes any warranty, express or implied, or assumes any legal liability or responsibility for the accuracy, completeness, or usefulness of any information, apparatus, product, or process disclosed, or represents that its use would not infringe privately owned rights. Reference herein to any specific commercial product, process, or service by trade name, trademark, manufacturer, or otherwise does not necessarily constitute or imply its endorsement, recommendation, or favoring by the United States Government or any agency thereof. The views and opinions of authors expressed herein do not necessarily state or reflect those of the United States Government or any agency thereof.

DISCLAIMER

Portions of this document may be illegible in electronic image products. Images are produced from the best available original document.

K^{*0} PRODUCTION IN K^+d INTERACTIONS AT 12 GeV/c*

A. Firestone, G. Goldhaber, and D. Lissauer

Department of Physics and Lawrence Radiation Laboratory
University of California, Berkeley, California 94720

August 1970

In this paper we report preliminary results on the interactions of 12-GeV/c K^+ mesons in deuterium. The SLAC 82-inch bubble chamber was exposed to an rf-separated 12-GeV/c K^+ meson beam. Resolution in the beam momentum to within $\Delta p/p = \pm 0.2\%$ is achieved by using the known correlation between beam momentum and transverse position in the bubble chamber.¹ Through the use of a gas Čerenkov counter, pion contamination in the beam is reduced essentially to zero. Approximately 500,000 exposures were taken, of which about 60% have been analyzed to date. The experimental details have been reported previously² in a study of the elastic charge exchange reaction $K^+n \rightarrow K^0p$. In the present paper we report on the charge exchange reactions ($K^+n \rightarrow K^+\pi^-p$ and $K^+n \rightarrow K^0\pi^+\pi^-p$.)

The film has been scanned for all events which have three-prong or four-prong topologies, both with and without associated V^0 decays. In addition, all measured four-prongs were required to have at least one track which stops in the bubble chamber. The events were measured on the LRL Flying-Spot Digitizer, and were reconstructed and kinematically fitted in the program SIOUX. For those events with invisible spectators (three-prongs), the spectator was assigned a momentum of zero with errors $\Delta p_x = \Delta p_y = \pm 30$ MeV/c, and $\Delta p_z = \pm 40$ MeV/c. All events which fit the four-constraint hypothesis, either $K^+d \rightarrow K^+\pi^-pp$ or $K^+d \rightarrow K^0\pi^+\pi^-pp$, with χ^2 probability greater than 0.1% were accepted.

The spectator proton (the slower proton in the laboratory frame) has a momentum distribution in agreement with that expected from the Hulthén wave function for momenta less than 300 MeV/c. For the subsequent analysis only events with $p_{\text{spect}} < 300$ MeV/c are accepted. There are 4260 and 510 such events for the reactions $K^+d \rightarrow K^+\pi^-pp$ and $K^+d \rightarrow K^0\pi^+\pi^-pp$ respectively, of which 67% are 3-prongs and 33% are 4-prongs in each case. The cross sections for these reactions have been determined to be 399 ± 8 μb for $K^+d \rightarrow K^+\pi^-pp$ and 212 ± 12 μb for $K^+d \rightarrow K^0\pi^+\pi^-pp$. Here the quoted errors reflect statistical uncertainties only.

1. GENERAL FEATURES OF THE REACTION $K^+n \rightarrow K^+\pi^-p$

Figure 1 shows the Dalitz plot for the reaction $K^+n \rightarrow K^+\pi^-p$. The outstanding features of this plot include the following: (1) a large low-mass enhancement in the $\pi\pi^-$ system, which is associated with several N^* resonances, (2) a $K^*(890)$ band, (3) a $K^*(1420)$ band, (4) a striking depletion of events in a band with $M^2(K^+\pi^-) \sim 2.4$ GeV^2 , (5) an excess of events asymmetrically distributed along a band with $M^2(K^+\pi^-) \sim 3$ GeV^2 , and (6) a general lack of background events. The Particle Data Tables list seven $N_{1/2}^*$ resonances with masses less than 1.8 GeV,³ several of which could contribute to the low-mass enhancement in the $\pi\pi^-$ distribution. Except possibly for some structure at $M^2(\pi\pi^-) \sim 2$ GeV^2 , which is probably associated with the P_{11} Roper resonance, none of them can be resolved without cuts in t . The Dalitz plot shows that, although there is perhaps some $K^*(1420)N^*$ and $K^*(890)N^*$ constructive interference, the N^* band is not continuous. The depletion of events in a band with $M^2(K^+\pi^-) \sim 2.4$ GeV^2 cuts right across the N^* band, and in addition the N^* band does not persist down to the region between the $K^*(890)$ and $K^*(1420)$. Moreover, the well-known asymmetry in the $K^*(890)$ decay angular distribution which appears

on the Dalitz plot as an asymmetric population density along the $K^*(890)$ band, appears not to be associated with the N^* ; i.e., the high density region of the $K^*(890)$ band is roughly the region with $M^2(p\pi^-) < 7 \text{ GeV}^2$, whereas the region attributable to the N^* is only the region with $M^2(p\pi^-) < 3 \text{ GeV}^2$.

Figure 2 shows the distribution in $M(p\pi^-)$ in which the N^* enhancement is very clear. Figure 3 shows the same $M(p\pi^-)$ distribution with cuts (a) $t < 0.3 \text{ (GeV/c)}^2$ and (b) $t > 0.3 \text{ (GeV/c)}^2$. The N^* peak is sharply shifted between the two; the P_{11} Roper resonance is apparently produced primarily at low t , while higher N^* 's are produced at higher t values.

II. $K_N^*(1250)$

Figure 4a shows the mass distribution $M(K^+\pi^-)$ for all the events in the sample. In addition to the features noted already, there is a sharp spike at a mass of $M(K^+\pi^-) = \underline{1250 \text{ MeV}}$. Figure 4b shows the data with the N^* peak removed ($M(p\pi^-) > 1.8 \text{ GeV}$) and the low t region selected ($t_{K \rightarrow K\pi} < 0.2 \text{ (GeV/c)}^2$). The enhancement is about 5 standard deviations above background in this distribution. A fit to the data of a Breit-Wigner line shape gives the following values for the parameters of this $K^*(1250)$ resonance, $M = 1247 \pm 5 \text{ MeV}$ and $\Gamma = 20_{-6}^{+9} \text{ MeV}$, with a $\chi^2 = 3.95$ for six degrees of freedom. The results of this fit are shown as a smooth curve in Fig. 2c. In a compilation by W. P. Dodd et al.,⁴ a K^* resonance at approximately this mass was observed; however, the width reported in that case was 70 MeV. If the large t region is selected, i.e., $t_{K \rightarrow K\pi} > 0.2 \text{ (GeV/c)}^2$, the $K^*(1250)$ does not appear significantly above the background, but there is some evidence for structure in the region $1 \text{ GeV} < M(K^+\pi^-) < 1.2 \text{ GeV}$. Evidence for two enhancements in this region have been reported; a $K^*(1080)$ (Ref. 5) and a $K^*(1160)$ (Ref. 6). However the statistical significance of any peaks in this region is marginal in the sample analyzed to date in this experiment.

Figure 5 shows the decay angular distributions, $\cos \theta$ and ϕ , and the distribution in momentum transfer, $t_{K \rightarrow K\pi}$ for the region of the $K^*(1250)$ and for two neighboring regions. The region of the $K^*(1250)$ has been defined as the 40-MeV band, 1.19-1.23 GeV (see Fig. 4c). The neighboring regions have also been taken as 40 MeV wide on either side of the $K^*(1250)$ region. The angle θ is the angle between the incident K^+ and the outgoing K^+ in the $K^+\pi^-$ rest frame (Jackson angle), and the angle ϕ is the azimuth of the outgoing K^+ about the incident K^+ axis in the $K^+\pi^-$ rest frame (Treiman-Yang angle). No cuts have been made in this data except for the indicated mass cut; specifically, $M(p\pi^-) > 1.8$ GeV has not been selected here, because such a cut is equivalent to a cut on θ , i.e., a cutting out of forward K^+ ($\cos \theta \sim +1$) events.

In the $K^*(1250)$ region, the distribution is consistent either with isotropy or with a polynomial in $\cos \theta$ of order 2. There is no evidence for any term in $\cos^n \theta$ where $n > 2$. We have fit the data to a function of the form $a_0 + a_1 P_1(\cos \theta) + a_2 P_2(\cos \theta)$, where the $P_i(\cos \theta)$ are the Legendre polynomials in $\cos \theta$. We obtain a $\chi^2 = 22.9$ for 17 degrees of freedom, and the best fit normalized parameters are $(a_1/a_0) = 0.28 \pm 0.19$ and $(a_2/a_0) = 0.86 \pm 0.22$. In the region below the $K^*(1250)$ there is no evidence for any deviation from isotropy, and in fact in that region we obtain parameters $(a_1/a_0) = 0.31 \pm 0.23$ and $(a_2/a_0) = -0.11 \pm 0.29$, but a fit to an isotropic distribution ($a_1 = a_2 = 0$) yields a $\chi^2 = 11.8$ for 19 degrees of freedom. In the region above the $K^*(1250)$ the data are consistent with isotropy, but there is some evidence for an asymmetry in this region; however this may be due to the effects of the tail of the $K^*(1420)$ which is becoming important at 1.3 GeV. The best fit parameters in this region are $(a_1/a_0) = 0.62 \pm 0.21$ and $(a_2/a_0) = 0.41 \pm 0.20$.

A least squares fit to the t distribution in the $K^*(1250)$ region (Fig. 5h) yields a slope of $12.5 \pm 1.5 (\text{GeV}/c)^{-2}$, which is certainly consistent with slopes

generally observed for pion exchange processes. If the $K^*(1250)$ is in fact produced primarily by pion exchange, then we may say that its spin-parity must be either $J^P = 0^+$ or 1^- , as there is no evidence for any terms higher than $\cos^2 \theta$ in the decay angular distribution. At the present level of statistics we cannot distinguish between $J^P = 0^+$ and $J^P = 1^-$, but the value $(a_2/a_0) = 0.86 \pm 0.22$ in the $K^*(1250)$ region tends to favor the $J^P = 1^-$ interpretation as this parameter would be zero for a $J^P = 0^+$ resonance produced by pion exchange. The $K^*(1250)$ does not have a large branching fraction into three-body final states. This is discussed in Section IV, where the reaction $K^+ n \rightarrow K^0 \pi^+ \pi^- p$ is studied.

III. EVIDENCE FOR A $J^P \neq 2^+$ SIGNAL ON THE LOW MASS SIDE OF $K^*(1420)$

In the $K^+ \pi^-$ mass distribution (see Fig. 4) we observe a rather broad signal from 1300 to 1500 MeV which appears to be due to the $K^*(1420)$ with $M \sim 1385$ MeV and $\Gamma \sim 140$ MeV. We note however that the character of the $K\pi$ decay angular distribution changes sharply at 1400 MeV. Figure 6 shows the $\cos \theta$ distributions where θ is the Jackson angle in the region of the $K^*(1420)$. The distribution in $\cos \theta$ for the high mass side 1400-1500 MeV (Fig. 6b) is just that distribution expected from the decay of a $J^P = 2^+$ object produced by pseudoscalar exchange. There is no evidence for any asymmetry, and the distribution may be fit with D waves with some S-wave background. The $\cos \theta$ distribution for the 1300-1400 MeV region, shown in Fig. 6a, can be fitted with S and P waves only and requires no D waves. This sharp change in character of the decay angular distribution can be further noted from Fig. 7 where we show the $K^+ \pi^-$ mass spectrum for three regions in $\cos \theta$: $0.7 < \cos \theta \leq 1$ (forward), $-0.7 < \cos \theta \leq 0.7$ (equatorial), and $-1 < \cos \theta < -0.7$ (backward) decay. We note that the entire " $K^*(1420)$ " peak appears in the forward region,

a peak at ~ 1360 MeV appears in the equatorial region, and a peak at ~ 1420 MeV appears in the backward region. One interpretation of this data would include the presence of a $J^P = 0^+$ or 1^- signal at ~ 1360 MeV with a width of $\Gamma \sim 60$ MeV in addition to the $K^*(1420)$. The possibility that a change in the character of the exchange mechanism at 1400 MeV is responsible for this effect appears to be unlikely in view of the fact that the t distributions for the two mass regions appear identical (see Fig. 8).

Further evidence for a sharp break at 1400 MeV can be seen in a comparison of the $(K^+\pi^-)$ mass distribution in this reaction with the $(K^0\pi^+\pi^-)$ mass distribution in the final state $K^0\pi^+\pi^-p$. This is discussed in Section IV.

We note that Antich et al.⁷ have previously suggested the presence of a $J^P = 1^-$ state, or at least an increase in the 1^- contribution to background, in the vicinity of $K^*(1420)$. This work is based on a study of the decay distributions of the $K\pi$ system in the reaction $K^+p \rightarrow K^+\pi^-\Delta^{++}$ at 5.5 GeV/c.

IV. $K^+n \rightarrow K^0\pi^+\pi^-p$

In Fig. 9 we show the distribution in $M(K^0\pi^+\pi^-)$ for the reaction $K^+n \rightarrow K^0\pi^+\pi^-p$. The most striking features of this distribution are the $K^*(1420)$ peak and the complete absence of any signal below the $K^*(1420)$. The well-known Q enhancement in $K\pi\pi$ is evidently not produced in a charge exchange reaction off the neutron as was noted earlier for other charge exchange reactions.^{8,9} The $K^*(1250)$ is also not produced in this reaction which indicates its branching ratio into three-body final states is small, and thus is not associated with the structure in the Q at about the same mass. We have calculated the ratio $R = (K^0\pi^+\pi^-)/(K^+\pi^-)$ as a function of the invariant mass of all the mesons in each final state, where the number of $K^0\pi^+\pi^-$ events have been corrected for the neutral decay mode and the K_2 decay of the K^0 . We note that in the 1280

to 1400 MeV mass region $R = 0.27 \pm 0.06$, while in the 1400 to 1520 MeV mass region $R = 0.60 \pm 0.09$. This is further evidence for the sharp change at 1400 MeV which cannot be explained by two-body and three-body phase space differences.

In addition, the $(K^0 \pi^+ \pi^-)$ mass distribution in Fig. 9b shows a peak at a mass of about 2.1 GeV. This peak is currently being investigated.

V. ACKNOWLEDGMENTS

We gratefully acknowledge the help of the SLAC accelerator operation group, and in particular we thank J. Murray, R. Gearhart, R. Watt, and the staff of the 82-inch bubble chamber for help with the exposure. We acknowledge the valuable support given by our scanning and programming staff, especially E. R. Burns, and H. White and the FSD staff.

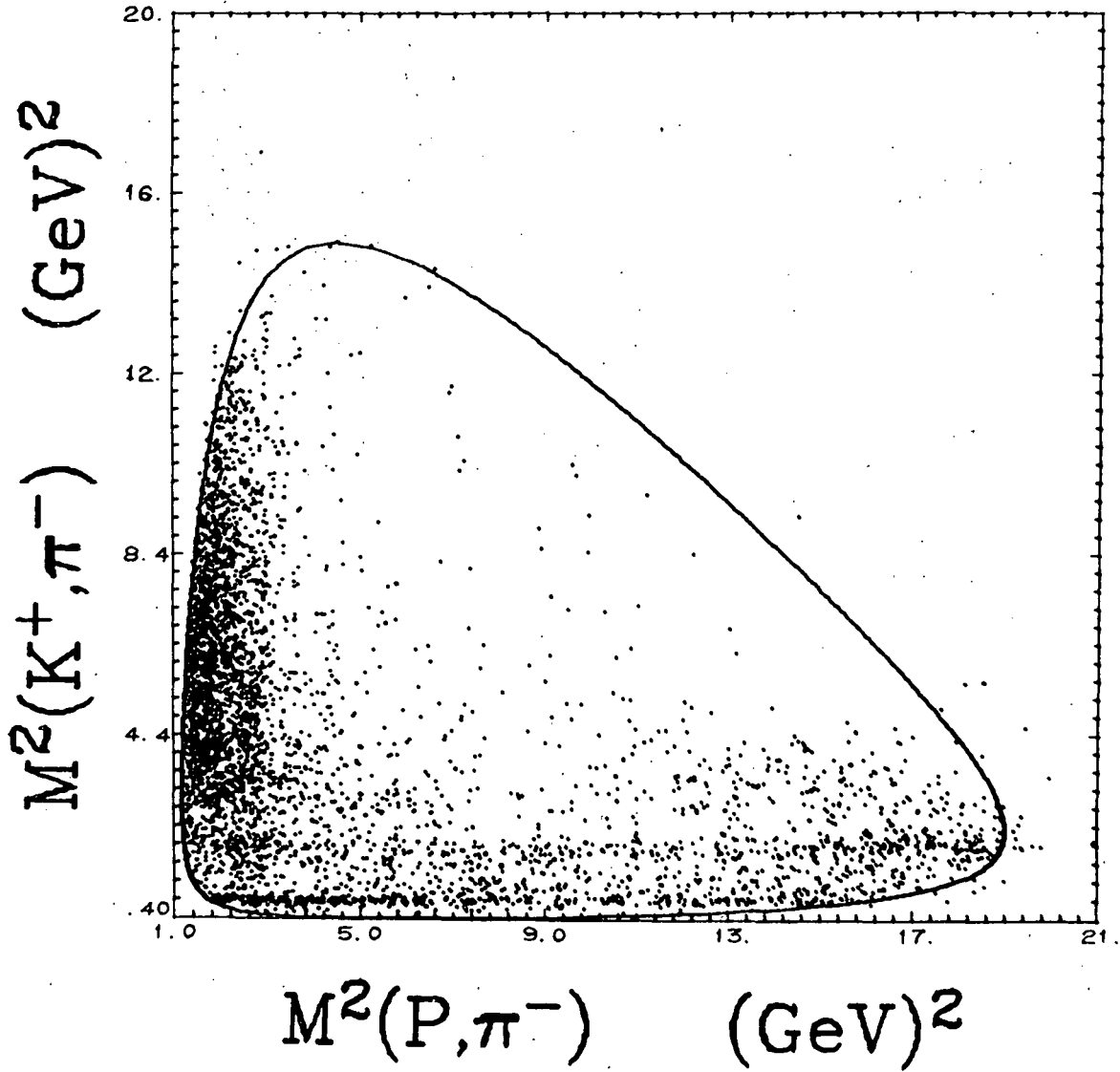
REFERENCES

*Work supported by the U.S. Atomic Energy Commission.

1. S. Flatte, LRL Berkeley, Group A Memo No. 664.
2. A. Firestone, G. Goldhaber, A. Hirata, D. Lissauer, and G. H. Trilling, UCRL-19880, submitted to Phys. Rev. Letters.
3. Particle Data Group, Review of Particle Properties, Rev. Mod. Phys. 42, 87 (1970).
4. W. P. Dodd, T. Joldersma, R. B. Palmer, and N. P. Samios, Phys. Rev. 117, 1991 (1969).
5. W. De Baere et al., Nuovo Cimento 51A, 101 (1967).
6. D. J. Crennell, U. Karshon, K. W. Lai, J. S. O'Neill, and J. M. Scarr, Phys. Rev. Letters 22, 487 (1969).
7. P. Antich et al., Phys. Rev. Letters 21, 842 (1968).
8. J. Bartsch et al., Phys. Letters 22, 357 (1966).
9. G. Alexander et al., Nucl. Phys. B13, 503 (1969).

FIGURE CAPTIONS

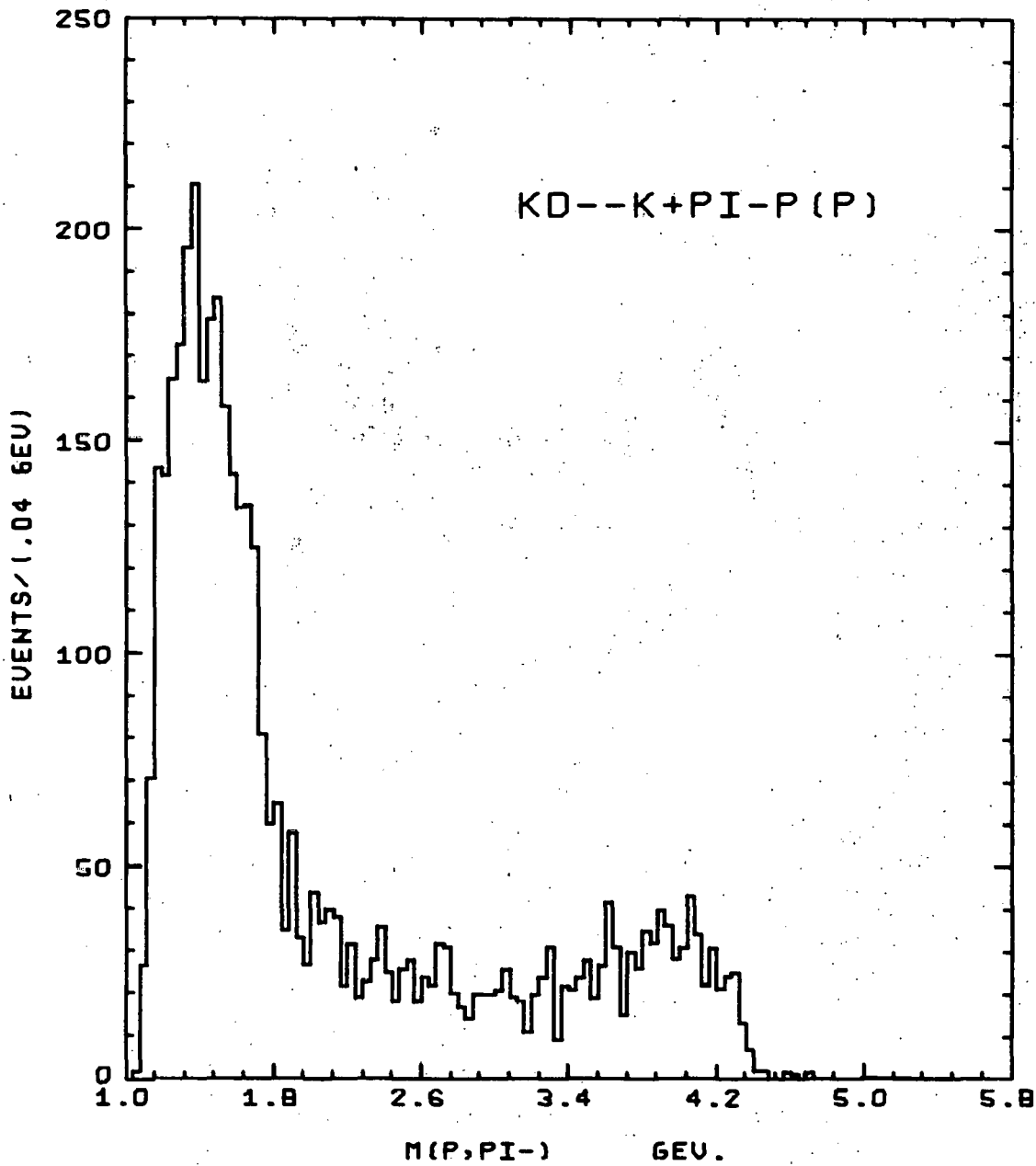
- Fig. 1. Dalitz plot $M^2(p\pi^-)$ vs $M^2(K^+\pi^-)$ for the reaction $K^+n \rightarrow K^+\pi^-p$.
- Fig. 2. $M(p\pi^-)$ for the reaction $K^+n \rightarrow K^+\pi^-p$.
- Fig. 3. $M(p\pi^-)$ for the reaction $K^+n \rightarrow K^+\pi^-p$ with (a) $t < 0.3$ (GeV/c)² and (b) $t > 0.3$ (GeV/c)².
- Fig. 4. $M(K^+\pi^-)$ for the reaction $K^+n \rightarrow K^+\pi^-p$ with (a) no cuts, (b) $M(p\pi^-) > 1.8$ GeV and $t_{K \rightarrow K\pi} < 0.2$ (GeV/c)², and (c) same as (b) in 10-MeV bins. The smooth curve in (c) is the result of a fit to a Breit-Wigner shape. See text.
- Fig. 5. (a) $\cos \theta$, the $K\pi$ decay angle, (b) ϕ , the Treiman-Yang angle, and (c) $t_{K \rightarrow K\pi}$ in three mass regions: (i) below the $K^*(1250)$, (ii) in the $K^*(1250)$, and (iii) above the $K^*(1250)$.
- Fig. 6. $\cos \theta$, the $K\pi$ decay angle for events in the $K^*(1420)$ region with (a) 1.3 GeV $< M(K^+\pi^-) < 1.4$ GeV and (b) 1.4 GeV $< M(K^+\pi^-) < 1.5$ GeV. The data have been selected with $t < 0.2$ (GeV/c)².
- Fig. 7. $M(K^+\pi^-)$ for (a) $0.7 < \cos \theta < 1$, (b) $-0.7 < \cos \theta < +0.7$ and (c) $-1 < \cos \theta < -0.7$. The data have been selected with $t < 0.2$ (GeV/c)².
- Fig. 8. $d\sigma/dt$ vs t for the low and high $K^*(1420)$ regions.
- Fig. 9. $M(K^0\pi^+\pi^-)$ for the reaction $K^+n \rightarrow K^0\pi^+\pi^-p$. The insert shows the same distribution with $M(p\pi^-) < 1.32$.



XBL 708-1783

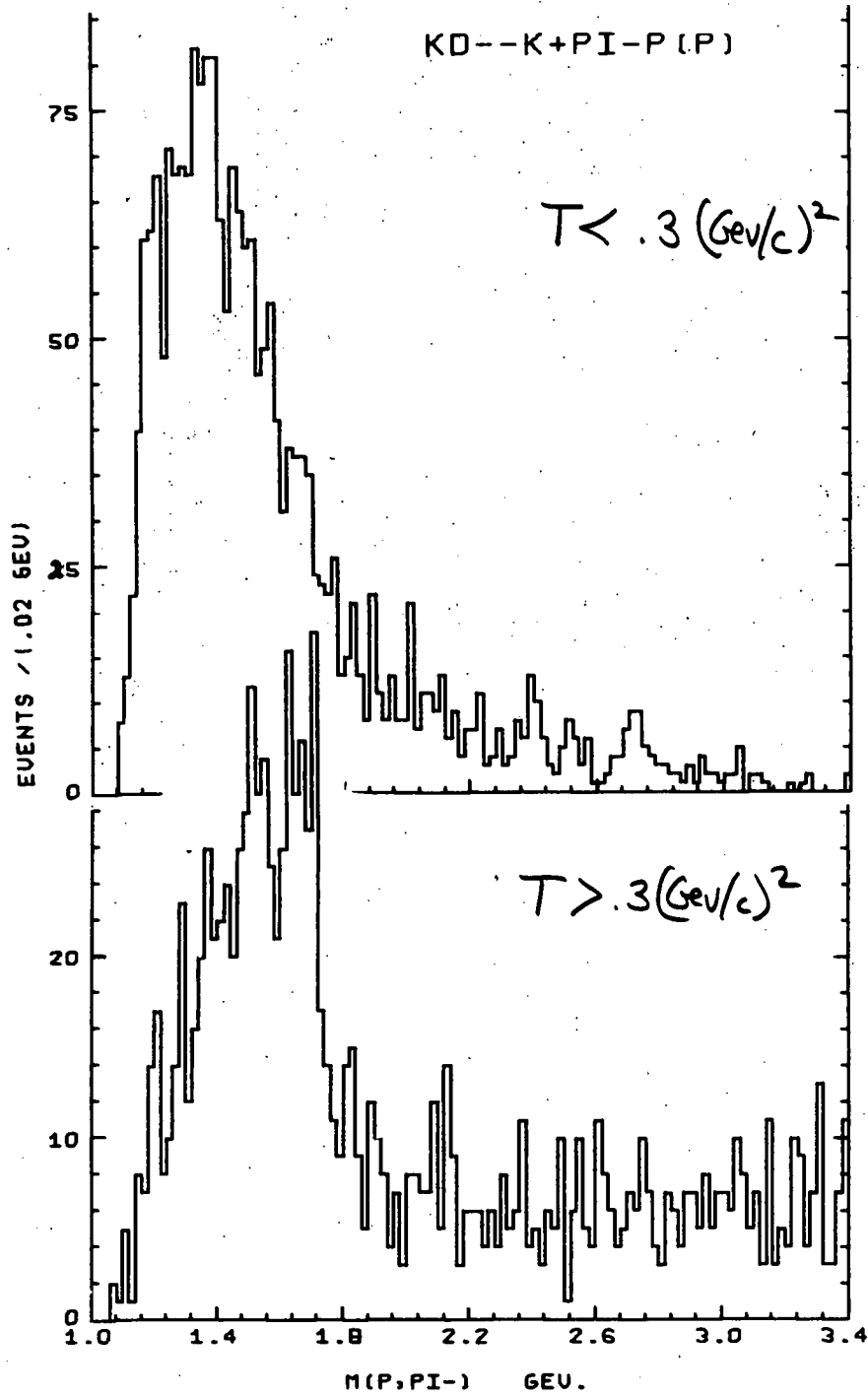
Fig. 1

MASS P,PI- ALL



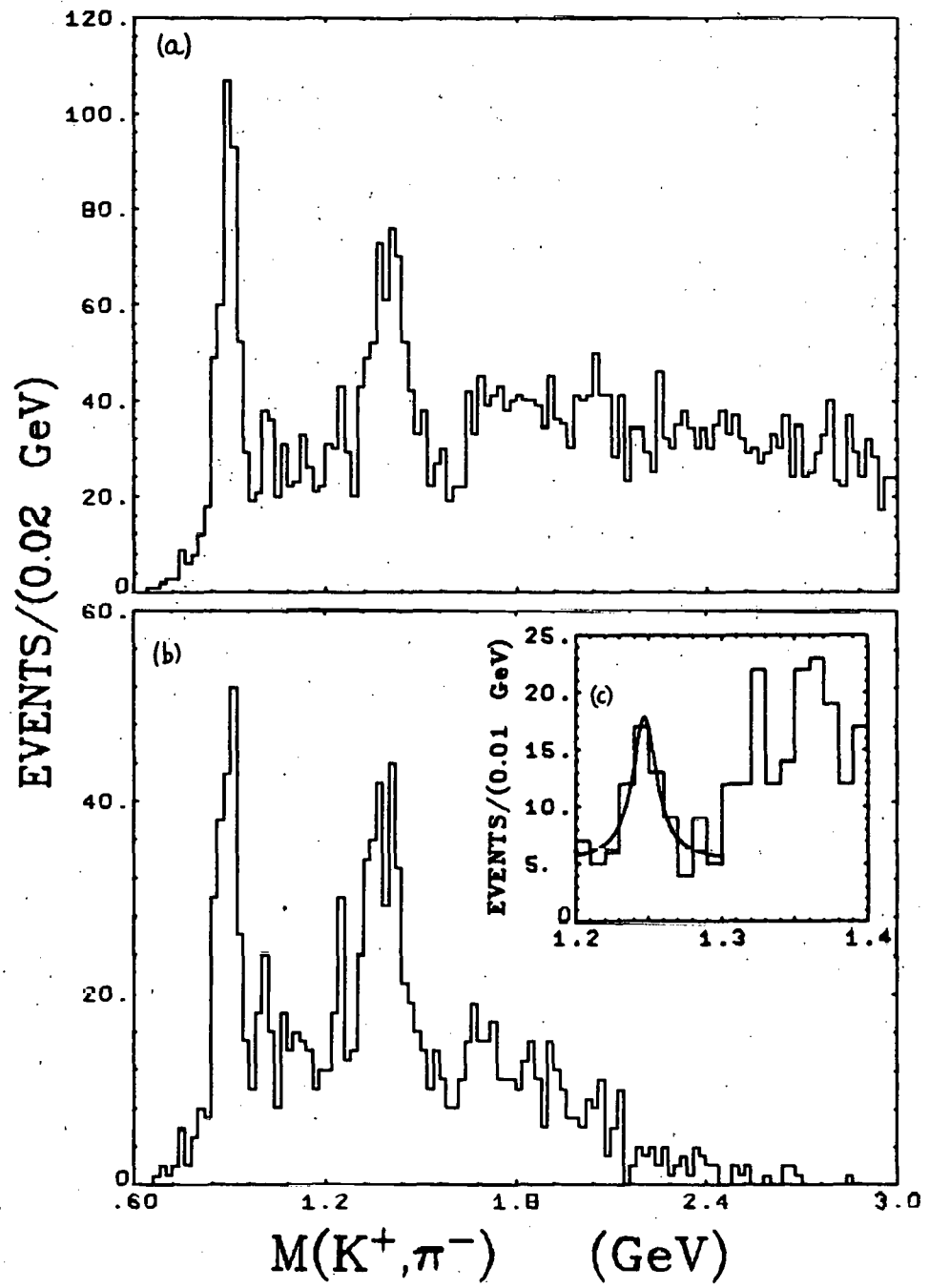
XBL 708-1807

Fig. 2



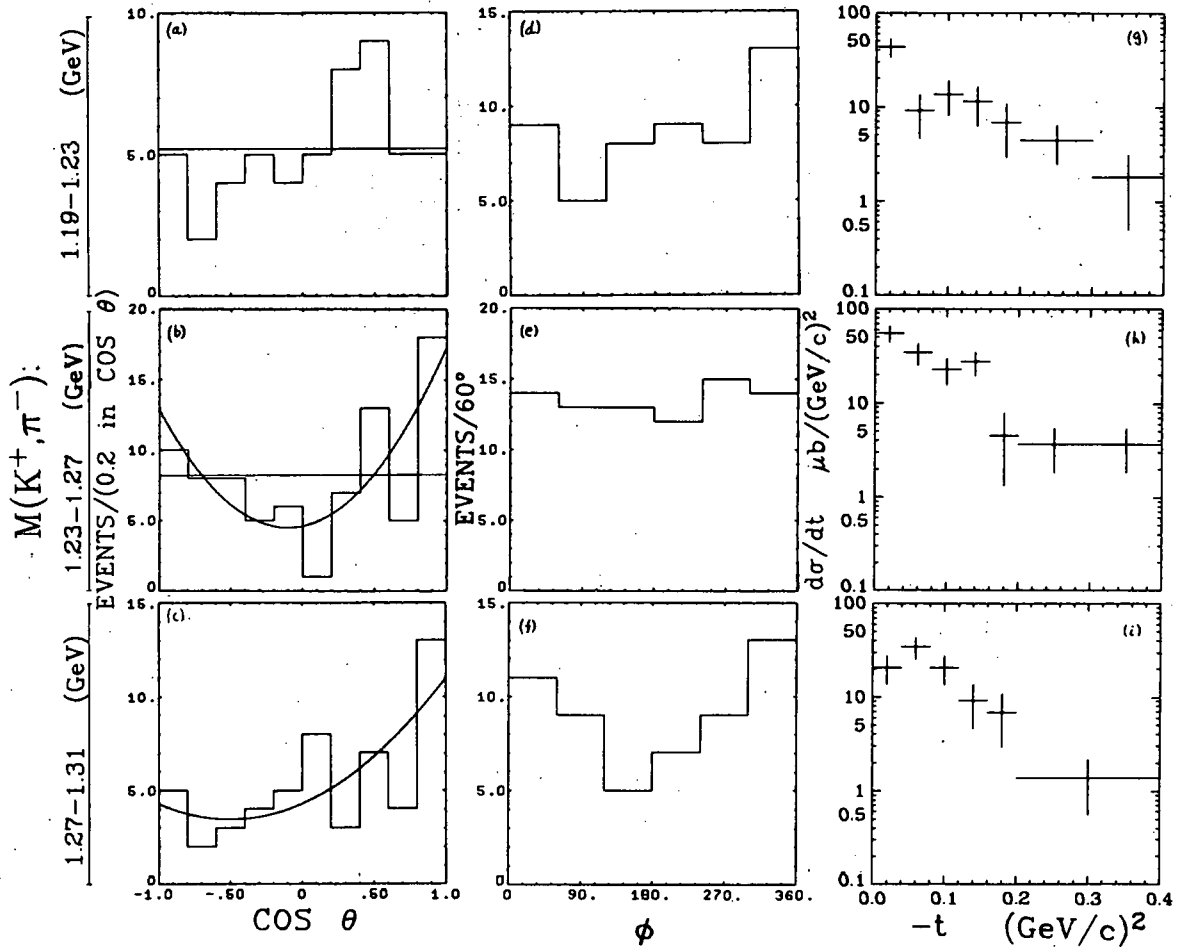
XBL 708-1802

Fig. 3



XBL 708-1782

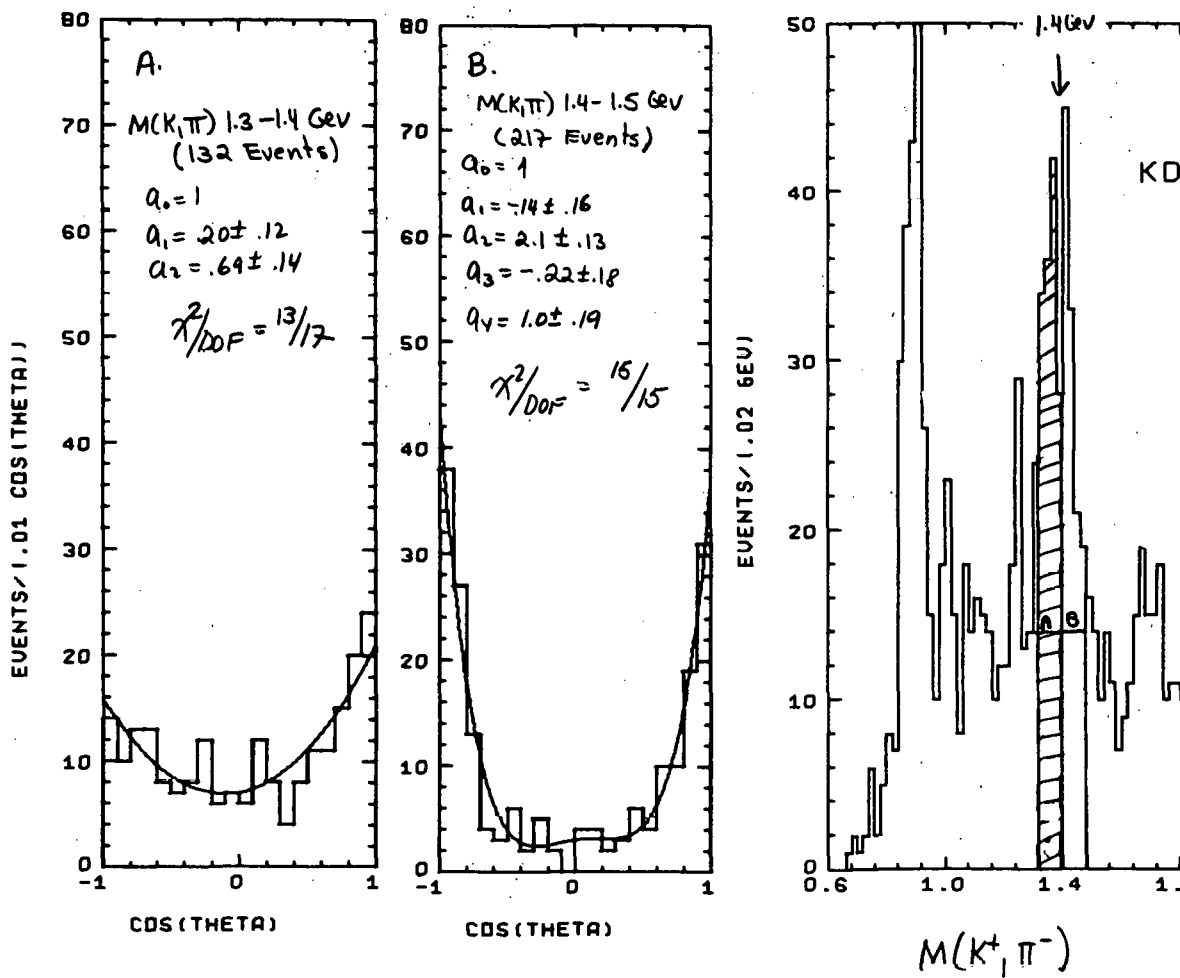
Fig. 4



XBL 708-1781

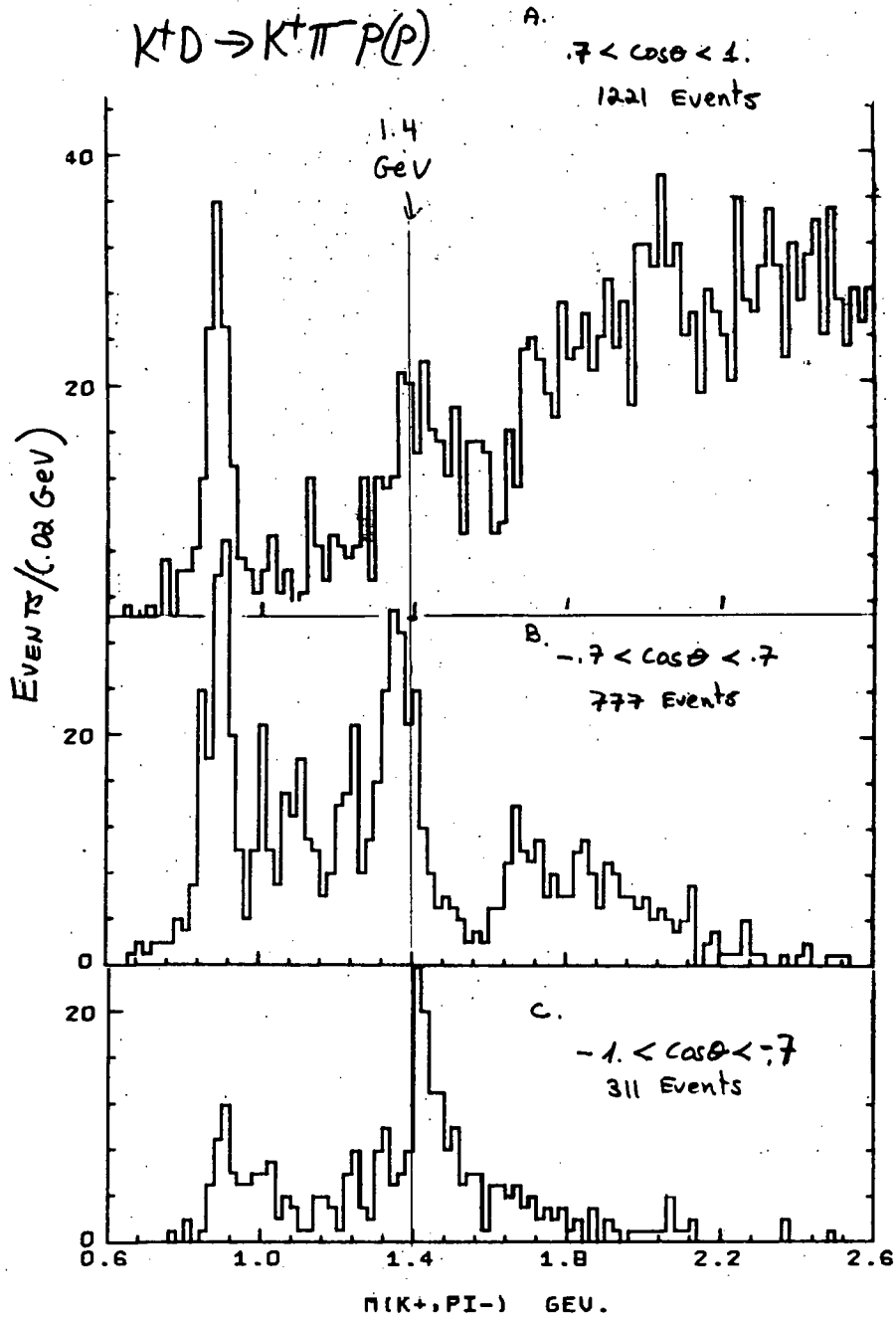
Fig. 5

$K^+ d \rightarrow K^+ \pi^- p(p)$ 12 GeV/c $|t| < 0.2 (\text{GeV}/c)^2$



XBL 708-1805

Fig. 6



XRI. 708-1A03

Fig. 7

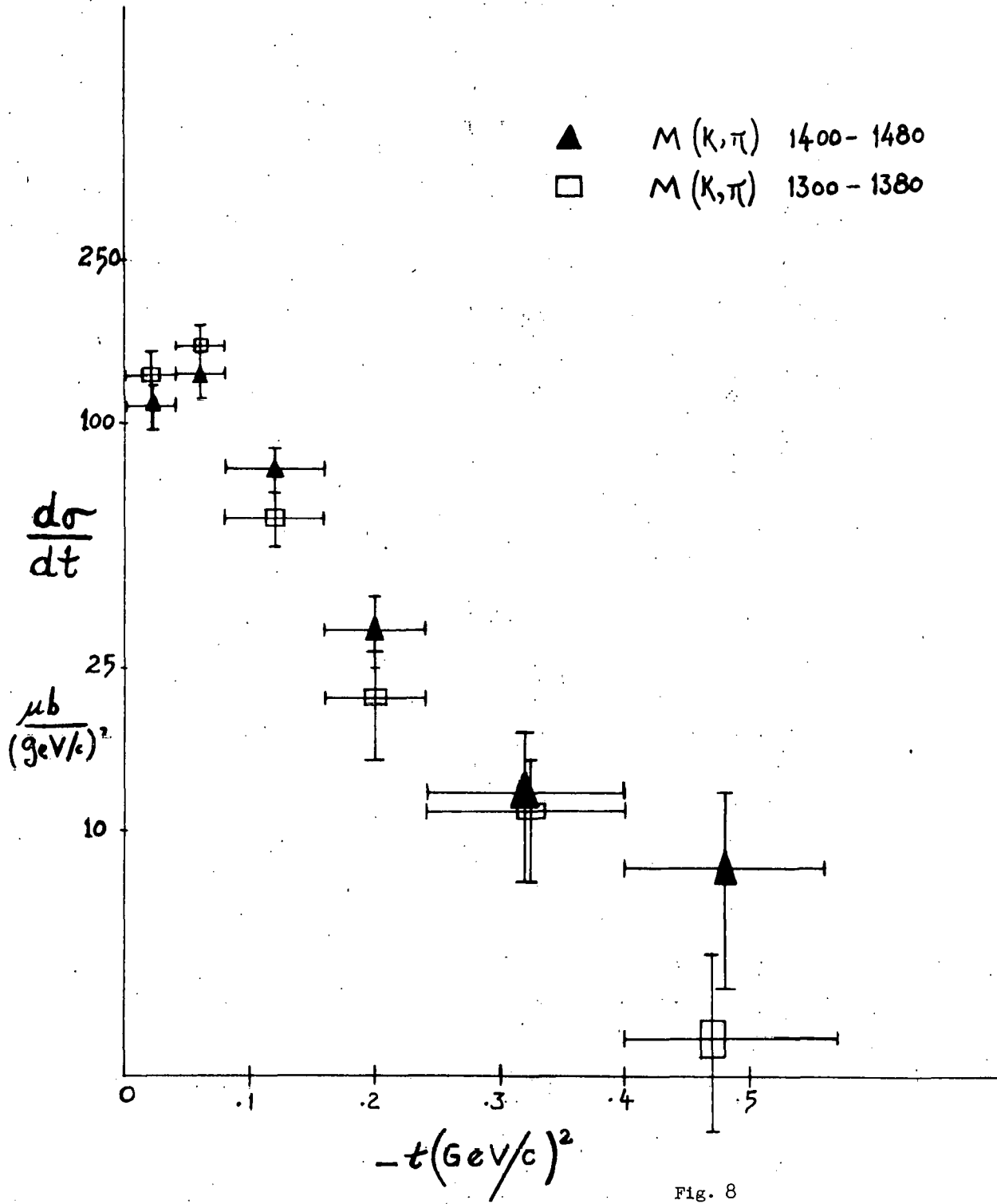
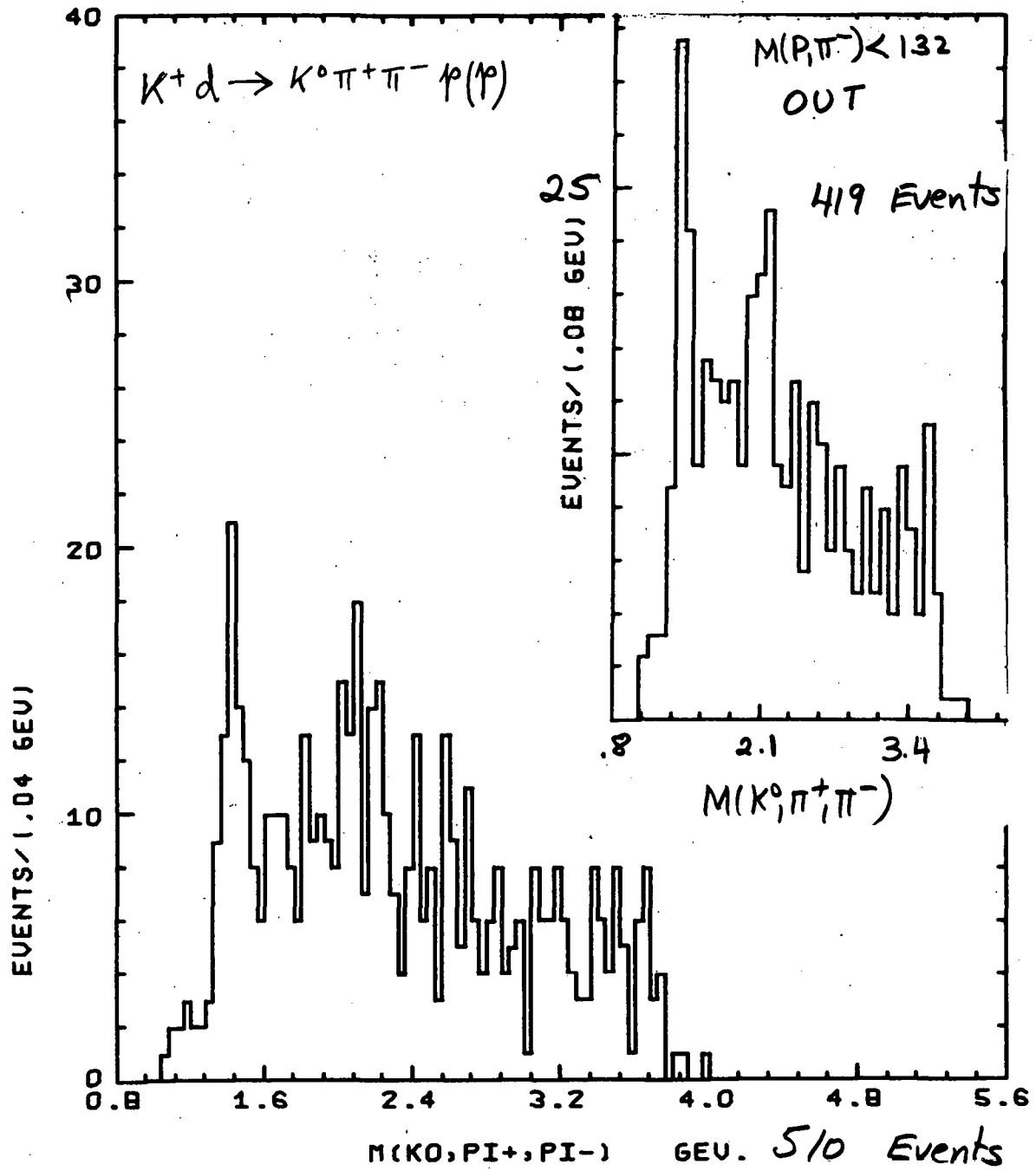


Fig. 8



XBL 708-1809

Fig. 9

LEGAL NOTICE

This report was prepared as an account of Government sponsored work. Neither the United States, nor the Commission, nor any person acting on behalf of the Commission:

- A. Makes any warranty or representation, expressed or implied, with respect to the accuracy, completeness, or usefulness of the information contained in this report, or that the use of any information, apparatus, method, or process disclosed in this report may not infringe privately owned rights; or*
- B. Assumes any liabilities with respect to the use of, or for damages resulting from the use of any information, apparatus, method, or process disclosed in this report.*

As used in the above, "person acting on behalf of the Commission" includes any employee or contractor of the Commission, or employee of such contractor, to the extent that such employee or contractor of the Commission, or employee of such contractor prepares, disseminates, or provides access to, any information pursuant to his employment or contract with the Commission, or his employment with such contractor.

TECHNICAL INFORMATION DIVISION
LAWRENCE RADIATION LABORATORY
UNIVERSITY OF CALIFORNIA
BERKELEY, CALIFORNIA 94720